Picosecond dynamics of a shock-driven displacive phase transformation in Zr

TD Swinburne,[1,*] MG Glavicic,[2] KM Rahman,[3] NG Jones,[4] J Coakley,[3,4,5] DE Eakins,[1] TG White,[1] V Tong,[3] D Milathianaki,[6] GJ Williams,[6] D Rugg,[7] AP Sutton,[1] and D Dye[3]

[1] *Department of Physics, Imperial College London, Exhibition Road, London SW7 2AZ, UK*
[2] *Rolls Royce Corporation, Indianapolis, IN 46206-0420, USA*
[3] *Department of Materials, Imperial College London, Exhibition Road, London SW7 2AZ, UK*
[4] *Department of Materials Science and Metallurgy, University of Cambridge, 27 Charles Babbage Road, Cambridge CB3 0FS, UK*
[5] *Department of Materials Science and Engineering, Northwestern University, 2220 Campus Drive, Evanston, IL 60208-3108, USA*
[6] *LCLS, SLAC National Accelerator Laboratory, Menlo Park, CA 94025, USA*
[7] *Rolls-Royce plc, Elton Rd., Derby, UK*

(Dated: March 29, 2016)

High pressure solid state transformations at high strain rates are usually observed after the fact, either during static holding or after unloading, or inferred from interferometry measurements of the sample surface. The emergence of femtosecond X-ray diffraction techniques provides insight into the dynamics of short-timescale events such as shocks. We report laser pump-probe experiments of the response of Zr to laser driven shocks over the first few nanoseconds of the shock event, enabling the $\alpha \rightarrow \omega$ transition and orientation relationship to be observed in real time with picosecond resolution. A clear orientation relationship of $(10\bar{1}0)_\alpha||(10\bar{1}1)_\omega$ is found, in conflict with $\omega \rightarrow \alpha$ annealing experiments in zirconium and the two $\alpha \rightarrow \omega$ pathways proposed for titanium.

The dynamics of materials subject to ultrafast shocks are of fundamental interest. At high strain rates deformation may be effected by the movement of interfaces during twinning and displacive phase transformations, in addition to conventional dislocation-mediated plasticity[1]. The $\alpha \rightarrow \omega$ phase transformation in hexagonal close packed metals is of particular importance because the high-pressure ω-phase is brittle, which may give rise to failure in metals that would be otherwise suited to a range of applications[2].

In this paper we report the first direct experimental observation of the $\alpha \rightarrow \omega$ phase transition in a hexagonal close packed metal, α-Zr, under shock conditions, employing recently developed[3–6] laser pump-probe experiments using the X-ray free electron laser (XFEL) to perform femtosecond X-ray diffraction (XRD) at the linac coherent light source of the Stanford linear accelerator center (CXI station, LCLS, SLAC). Pump-probe experiments use a femtosecond XFEL pulse to take an XRD snapshot (the probe) at a precise time delay after a shock pulse from an optical laser (the pump). By repeating this operation on statistically equivalent samples a time-ordered data set is produced, yielding a dynamic representation of the shock response.

I. INTRODUCTION

Despite significant theoretical and experimental investigation[1,7–11] the pathway of the $\alpha \rightarrow \omega$ transformation under shock is unresolved. Shock recovery experiments[1,9,11,12] can investigate only the isothermal, quasistatic $\omega \rightarrow \alpha$ transformation, by annealing previously shocked samples with significant regions of quenched ω-phase to recover the low pressure α-phase, whilst tracking the crystallographic texture during annealing through the variation of X-ray diffraction (XRD) peaks with sample orientation[13]. In this way the orientation relation (OR) between the α and ω phases can be extracted. In the majority of such experiments, one of two orientation relationships were identified: 1) an OR of $(0001)_\alpha||(11\bar{2}0)_\omega$ was found, consistent with the transformation pathway proposed by Silcock for Ti[7], which suggests $(0001)_\alpha||(11\bar{2}0)_\omega$, $[11\bar{2}0]_\alpha||[0001]_\omega$[11]. Alternatively, 2) an OR of $(0001)_\alpha||(10\bar{1}0)_\omega$ in agreement with a pathway found from *ab initio* calculations in Ti[2] that suggests $(0001)_\alpha||(10\bar{1}1)_\omega$, $[11\bar{2}0]_\alpha||[\bar{1}011]_\omega$. There is also experimental evidence for a dense array of $[0001]_\alpha$ dislocations surrounding a nucleated ω-phase region[8].

Because shocks are rapid, adiabatic events, the quasistatic, isothermal $\omega \rightarrow \alpha$ transformation observed during annealing in shock recovery experiments is not required to follow the same pathway as the shock-driven $\alpha \rightarrow \omega$ transformation. The isothermal, quasistatic conditions of the reverse transformation could result in a reconstructive, rather than displacive, transformation mechanism. One route to understanding shock-driven transformations are molecular dynamics (MD) simulations, which can treat up to tens of millions of atoms as classical particles interacting through an interatomic potential. Whilst an interatomic potential suitable for shock-driven dynamics in Zr is not currently available, recent MD simulations of shocked Ti[14] have found 1) an OR of $(0001)_\alpha||(10\bar{1}0)_\omega$ for shocks along $[0001]_\alpha$, transforming through a shuffle-strain mechanism along $[10\bar{1}0]_\alpha$, and 2) an OR of $(10\bar{1}0)_\alpha||(11\bar{2}0)_\omega$ for shock along $[11\bar{2}0]_\alpha$, in which the α-phase first transformed

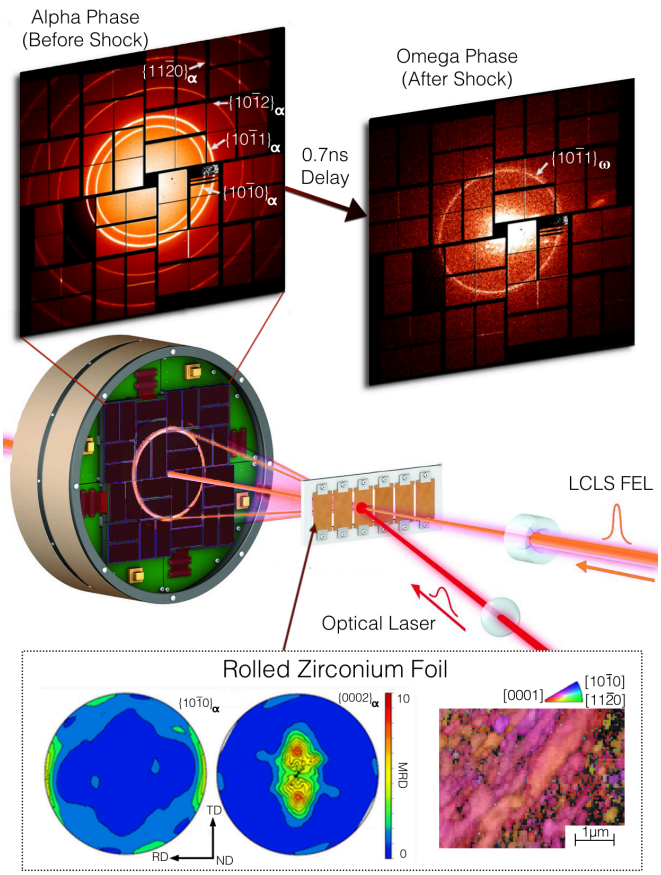

FIG. 1. Above: Typical XFEL diffraction data before and after the laser pulse. Shortly after the shock, the α-Zr rings are observed to disappear, being replaced by a weak, broad $\{10\bar{1}1\}_\omega$ ring. Center: Experimental arrangement. The XFEL beam impinges on the Zr foil sample shortly after a laser shock pulse, with the diffraction data recorded in transmission geometry. Below: Sample pole figures[15] for the Zr foils in equal area projection. Scale is in multiples of a random distribution (MRD). EBSD measurement revealed a modal grain size of $\sim 0.1\mu m$.

to an intermediate structure through a rotation of 90° around $[11\bar{2}0]_\alpha$ before transforming to the ω-phase by the Silcock mechanism. The ω-phase was accommodated through incoherent twin boundaries with the α-phase[14]. In both cases the observed ORs were in conflict with shock recovery measurements in Ti, highlighting the need for experimental measurement of shock-driven $\alpha \rightarrow \omega$ transitions.

II. LASER PUMP-PROBE EXPERIMENTS

Polycrystalline cold rolled Zr foils of 99.9% purity and 2μm in thickness were bonded to 100 μm-thick, optically polished, 25mm×40mm Si $\langle 100 \rangle$ substrates, with a glue layer less than 1μm thick. The commercially pure foils had an impurity content of 0.1%, well below levels which are known to affect phase transitions under dynamic loading[10]. XRD texture measurements were made using a Philips XPert MRD machine in texture configuration via the back reflection technique using copper K_α radiation. Intensities up to an incident angle of 80° from the sample normal were measured, with a defocussing correction, followed by a spherical harmonic and then WIMV analysis to construct equal-area projection pole figures using the popLA texture analysis software[15]. The reconstructed pole figures (Figure 1), show a typical cold rolled texture, with the (0002) poles at an angle of $\sim \pm 25°$ to the normal direction (ND) towards the transverse direction (TD) and a strong $\{10\bar{1}0\}$ texture in the rolling direction. This is a consequence of $\{10\bar{1}0\}\langle 11\bar{2}0\rangle$ slip being the easiest slip system in Zr. EBSD measurement found a modal grain size of $\sim 0.1\mu$m (Figure 1).

An array of six zirconium-coated silicon substrates were placed on the cassette shown in Figure 1. The optical shock pulses had a spatial separation of 3 mm with a spot size of $500-130\mu$m, depending on the desired pulse power, whilst the XFEL ($\lambda = 1.291$Å) had a spot size of 30μm. This meant that all the diffraction data was taken from well inside the shocked area, avoiding complications of a heterogeneous stress state across the foil surface. In addition, variations in the shot-to-shot granular stress state are suppressed as each diffraction pattern is an average across the 100-1000 grains within each XFEL spot.

The XFEL beam was at normal incidence to the foil, with the diffraction data recorded in transmission geometry using the CSpad X-ray detector[16]. The XFEL and optical laser were operated in burst mode, and their temporal overlap in the interaction region was set to within ±20ps, such that $t = 0$ corresponded to overlap of their leading edges. The pulse profile was a spectrally-shaped Gaussian, with a linear rise to 90% intensity of 80ps, and a FWHM of 170ps. Once relative timing was set, the average error in synchronization was ∼160fs, with a standard deviation in the shot-to-shot power of 0.015%. Before each laser pulse 600 XRD images were recorded and averaged to measure accurately the pre-shock state, whilst a single XRD image was taken after the optical laser pulse. At each optical laser power the pump-probe delay was systematically increased from zero in increments of 50 ps to obtain a time-ordered dataset.

The Zr foils were subjected to shocks of three intensities. The results are shown in Figure 2. It was found that with increasing shock power a new diffraction peak emerged, heralding a complete transformation of the diffraction pattern at the highest pump power, which we identify as the $\alpha \rightarrow \omega$ transition. The compressive shock wave took approximately 0.4ns to traverse the sample; by 0.7ns the reflected tensile wave resulted in a

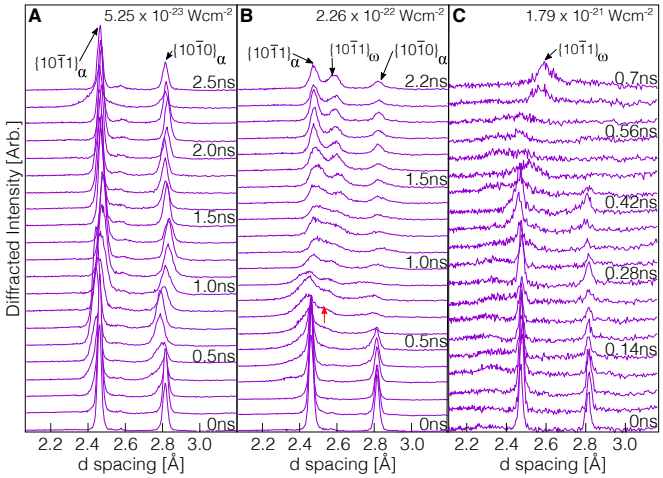

FIG. 2. XRD patterns before and after a laser shock at increasing shock power, with peak laser intensities of a) 5.25×10^{-23}Wcm^{-2}, b) 2.26×10^{-22}Wcm^{-2} and c) 1.79×10^{-21}Wcm^{-2}. The planes giving rise to the peaks are identified and the red arrow in b) signifies the emergence of the new ω peak.

through-thickness average of zero pressure, followed by a period of tension, and so on, with strong attenuation due to transmission to the Si substrate.

III. EXPERIMENTAL RESULTS

At the lowest shock power (Figure 2a) no phase changes were observed after the shock had passed. As the incident X-rays strike the foil along the foil normal, the relative changes in peak position are a result of changes in the through-thickness average of elastic strains transverse to the shock pulse. During the low power shock, Figure 3a, first an interval of compression was observed, followed by tension, and these returned to zero $\sim$ 2.5ns after the shock. The rise in peak width during the shock event is a result of both the through-thickness averaging of strain, and the generation of defects such as dislocations and their associated strain fields[17].

At medium shock power (Figure 2b) a new peak appeared gradually, along with significantly larger peak broadening during the shock (Figure 2b inset). At the same time, the measured lattice strains in the α-Zr peaks did not return to zero (Figure 3b), in particular for the $\{10\bar{1}1\}_\alpha$ and $\{10\bar{1}2\}_\alpha$ reflections. This is consistent with the Burgers vector of any induced dislocations being predominantly along basal directions, as the $\{10\bar{1}0\}_\alpha$ reflection is not sensitive to the spacing of basal planes.

At the highest shock power the peaks due to the α-phase eventually disappeared completely, leaving only a new peak in an identical position to that found at medium shock power (Figures 2c). The disappearance of peaks from the α-phase, leaving only the new peak, indicates that the material has undergone a phase change.

The identification of the new peak (observed at $d = 2.60 \pm 0.07$Å) following shock was made using zero pressure lattice parameters[18] for the α and ω-crystal structures in Zr. A planar spacing of $d = 2.60 \pm 0.07$Å in Zr is consistent with either the $\{0002\}_\alpha$ reflection at $\sim 1\%$ tension (from $d = 2.57$Å) or the $\{10\bar{1}1\}_\omega$ reflection at $\sim 2\%$ compression (from $d = 2.64$Å).

For the new Zr peak to be the $(0002)_\alpha$ reflection, one would require the shocked α-phase in the highly textured foil to undergo a rotation of around 90° to the foil normal such that the basal planes come into diffraction along the periphery of the pole figures. Although such a reorientation is possible by the twinning / rotation mechanism described by Zong *et al.*[12], these mechanisms are highly unlikely for two primary reasons. Firstly, the threshold twinning stress in Zr is around 100MPa at room temperature[19] and thus we would expect to see evidence of such mechanisms at all laser shock powers, not just the intermediate and highest laser power. This is contrary to what was observed, Figure 2a, thus providing direct evidence against this mechanism being responsible. Secondly, at the highest shock power the entire diffraction pattern was transformed into a single peak (Figure 2c). If this transformation were achieved by twinning or a reorientation mechanism, the entire shocked sample would then have to undergo a macroscopic rotation which places all of the crystallites in a configuration suitable for only the $\{0002\}_\alpha$ peak to be oriented for diffraction. This is an implausible explanation in that twinning mechanisms rely upon the twin being created within a parent orientation that would persist in the shocked sample. Correspondingly, the post shock diffraction pattern should still contain evidence of the parent orientation, albeit at lower intensities. The lack of any intensity relating to the parent phase suggests that the material is behaving differently under shock loading. As a result, we conclude that the new peak is a $\{10\bar{1}1\}_\omega$ reflection. As our pump probe experiments are destructive we cannot analyze samples post-shock, but a phase change is expected under similar conditions from previous shock recovery experiments[12].

At both the intermediate and highest shock powers, the ω-phase peak was identifiable just after the point of maximum compressive strain, at approximately 0.5ns. However, it is likely that the ω-phase was first present at the point of maximum compressive strain, obscured due to the large width of the diffraction peaks at this point (c.f. Figure 3b, inset). At later times the ω-phase peak appears to grow and narrow monotonically, which we attribute to an increasingly homogeneous stress state

in the ω-phase rather than an increasing volume of the transformed region. Owing to variations in stress state through the foil thickness, the time taken for the appearance of the ω-peak cannot be directly equated to the time for the transformation but at the highest laser power the entire shocked region transformed to the ω-phase in less than 0.4ns, consistent with a shear wave speed of $\sim 5\text{kms}^{-1}$ in Zr[20].

IV. SHOCKED MATTER SIMULATIONS

Our experimental results were compared to shockwave simulations using the hydrodynamic code HYADES[21], which balances energy, momentum and mass with respect to SESAME[22] equations of state for Zr and Si. Although HYADES is not sensitive to crystallographic orientation we are able to account for attenuation due to the Zr-Si impedance mismatch and obtain an estimate of the longitudinal strain in the Zr foil, which can then give estimates of the stress state during the shock, using a perfectly plastic strength model with a yield stress for Zr of 420 MPa. The time resolved longitudinal strains from these simulations are shown in Figure 3b), which show good agreement with the experimentally observed lattice strains data until approximately 1ns. After 1ns an additional oscillation is predicted but not observed, implying the simulations underestimate the degree of transmission of the shock wave to the substrate, but are able to characterize initial 1ns well.

The HYADES simulations gave peak longitudinal stresses of 3.8GPa, 7.6GPa and 22.1GPa at low, intermediate and highest shock power, where in experiment the $\alpha \rightarrow \omega$ transition was absent, partial and complete. The stress values of 3.8GPa and 7.6GPa therefore give lower and upper bounds for the $\alpha \rightarrow \omega$ transition stress, in good agreement with previous measurements in pure zirconium[23] that found a threshold stress of 6.8GPa for the $\alpha \rightarrow \omega$ transition, with partial transformations seen above 5GPa. A higher threshold stress of 10.6GPa has been estimated in the zirconium alloy E110[24], consistent with known alloying effects on the $\alpha \rightarrow \omega$ transition in titanium[10].

V. ORIENTATION RELATION BETWEEN α AND ω PHASES

The significant azimuthal variations of the intensities of the $\{10\bar{1}0\}_\alpha$ and $\{10\bar{1}1\}_\alpha$ diffraction rings, present due to the pronounced basal texture of the foil (Figure 1 inset), gives valuable information on the orientation of the diffracting α and ω lattice planes during the shock[13]. Lattice planes in the diffraction condition in transmission geometry have normal directions at a large angle to the foil normal, meaning their reflections are

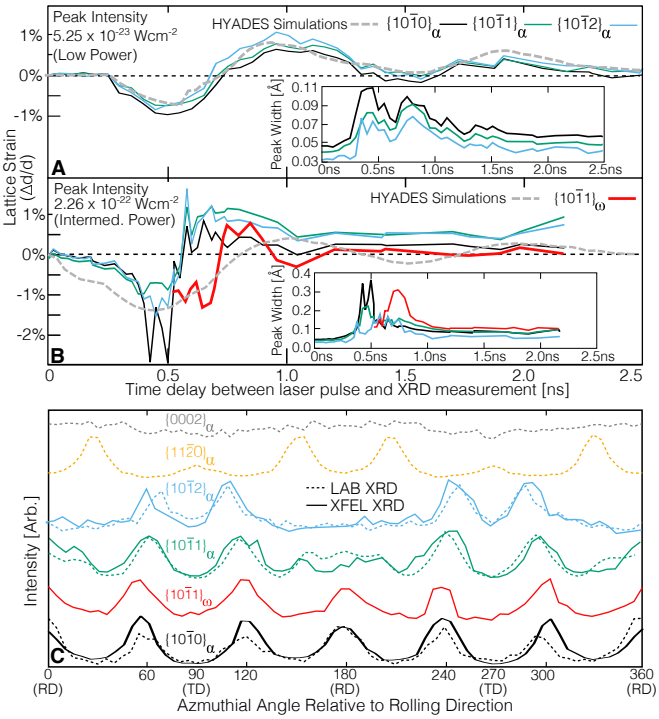

FIG. 3. Time resolved (data every 50 ps) response of Zr foils to a laser shock. Two upper panels: Strain as inferred from position of diffraction peaks for a) lowest laser power (peak intensity of $5.25 \times 10^{-23}\text{Wcm}^{-2}$) and b) medium laser power (peak intensity of $2.26 \times 10^{-22}\text{Wcm}^{-2}$). The dashed grey lines are the output of our HYADES simulations. Insets: FWHM of diffraction peaks. The strain and width of the $\{10\bar{1}1\}_\omega$ peak are referenced to the final steady state, whilst for the α-phase they are referred to the un-shocked state. c) Normalized XRD intensities for the α-peaks and the ω-peak at the end of the shock event (solid line: XFEL data at medium laser power, dotted line: reconstruction from laboratory XRD PFP). It is seen that the $\{10\bar{1}1\}_\omega$ texture corresponds to the parent $\{10\bar{1}0\}_\alpha$.

near the periphery of the pole figures in Figure 1. As the pole figures were constructed from separate XRD measurements of the same foil, we can calibrate XFEL measurements of the α phase with the independent XRD measurements taken to construct the pole figure periphery (PFP). Once calibrated, we can then compare the XFEL measurements of the α and ω phases in order to construct a partial orientation relation for the $\alpha \rightarrow \omega$ transformation under shock conditions.

As shown in Figure 3c, the strong basal texture of the Zr foil is evidenced by the independence of the intensity of the $(0002)_\alpha$ reflection on the azimuthal angle, and by the evident six-fold symmetry for the other planes. As expected, the $\{11\bar{2}0\}_\alpha$ reflection has peaks at 30° to $\{0\bar{1}n\}_\alpha$ reflections. The XFEL data, which shows excellent agreement with the PFP data, is an aggregate of all individual diffraction patterns for the α-phase before and after the XFEL pulse. The data for the

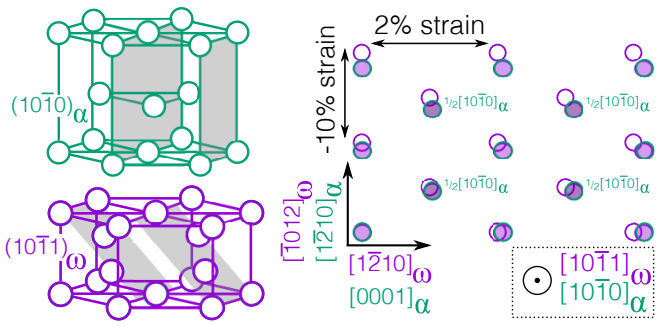

FIG. 4. Illustration of the observed orientation relationship $(10\bar{1}0)_\alpha||(10\bar{1}1)_\omega$. Left: $(10\bar{1}0)_\alpha$ and $(10\bar{1}1)_\omega$ planes highlighted in their respective lattices. Right: Superposition of $(10\bar{1}0)_\alpha$ and $(10\bar{1}1)_\omega$ planes. Upon aligning $[0001]_\alpha$ and $[1\bar{2}10]_\omega$, the atomic positions on $(10\bar{1}0)_\alpha$ planes can be brought into coincidence with atomic positions on $(10\bar{1}1)_\omega$ planes after a homogeneous strain, giving a potential full orientation relation of $(10\bar{1}0)_\alpha||(10\bar{1}1)_\omega$, $[0001]_\alpha||[1\bar{2}10]_\omega$.

ω-phase peak is an aggregate of all the diffraction data around 1.4 ns after the laser pulse where a steady state was observed, as shown in Figures 2-3. Inspection of Figure 3 demonstrates that both the periodicity and intensity of the $\{10\bar{1}1\}_\omega$ reflection are aligned with the $\{10\bar{1}0\}_\alpha$ reflection, giving a clear orientation relationship of $\{10\bar{1}0\}_\alpha||\{10\bar{1}1\}_\omega$.

VI. DISCUSSION

The measured orientation relationship is not compatible with the two $\alpha \rightarrow \omega$ pathways reported in the literature, Silcock[7] and TAO-1[2]. Whilst these pathways were originally developed for titanium, they have been employed to interpret the $\alpha \rightarrow \omega$ transition in zirconium[12], and to our knowledge no other $\alpha \rightarrow \omega$ transition pathways have been proposed for Zr. By considering the effect of the full transformation pathway[25] on pairs of vectors lying in the three possible $\{10\bar{1}1\}_\omega$ planes, we found the Silcock pathway predicts $\{10\bar{1}1\}_\omega$ planes should be approximately aligned with $(1\bar{3}20)_\alpha$, $(0\bar{2}23)_\alpha$ and $(1\bar{1}03)_\alpha$ planes. As quoted above, the TAO-1 pathway predicts $(0001)_\alpha||(10\bar{1}1)_\omega$, whilst the two other $\{10\bar{1}1\}_\omega$ planes should be approximately aligned with $(11\bar{2}3)_\alpha$ and $(1\bar{2}13)_\alpha$ planes. In both cases, all the possible orientation relationships are incompatible with the orientation relationship $(10\bar{1}0)_\alpha||(10\bar{1}1)_\omega$ seen in our experiments.

The observed orientation relationship is illustrated in Figure 4. Whilst we do not propose a transformation pathway between the two phases, we have found that the atomic positions in the α-phase, when projected onto $(10\bar{1}0)_\alpha$ planes, may be brought into coincidence with the atomic positions of $(10\bar{1}1)_\omega$ planes, providing $[0001]_\alpha$ and $[1\bar{2}10]_\omega$ directions are aligned. Using equilibrium lattice parameters for the α and ω phases in Zr[18], the atomic positions in the two planes may be brought into coincidence via a tensile strain of approximately 10% along $[1\bar{2}10]_\alpha$ and a compressive strain of approximately 2% along $[0001]_\alpha$. Clearly, further theoretical investigation is needed to determine a potential transformation pathway that can accommodate these large tensile strains, but we note that if such a pathway can be found, the full orientation relationship for the $\alpha \rightarrow \omega$ transformation would be $(10\bar{1}0)_\alpha||(10\bar{1}1)_\omega$, $[0001]_\alpha||[1\bar{2}10]_\omega$.

The $\alpha \rightarrow \omega$ transformation pathway has implications for how HCP metals respond to shock loads. We have provided strong evidence that the $\alpha \rightarrow \omega$ transformation in Zr under shock loading conditions is quite different to that measured in isothermal, quasistatic experiments in Zr and *ab initio* calculations in Ti. Whilst further theoretical and experimental work is needed on the known orientation-dependence of shock-driven transformations, the picosecond timescales of the pump-probe experiments reported here are directly comparable to modern simulation techniques. However, by searching for a minimum energy transformation path, current *ab initio* calculations attempt to estimate the most likely quasistatic transformation pathway with no accommodation of thermal vibrations. Our results suggest that non-equilibrium concepts, such as basins of attraction in configurational phase space[26], may give insight into the role of entropy in predicting the response of crystalline materials to shock loads.

VII. CONTRIBUTIONS

DR, MGG and APS conceived the experiment and secured beam time. DD, MGG, DE, KMR and DM designed the experiment and selected appropriate materials. DM, TDS, KMR, NGJ, JC and MGG performed the experiment at the XFEL. NGJ and TDS performed initial analysis of the XFEL X-ray data. KMR and VT performed microstructural characterisation of the starting materials. DE, TW and JC performed additional analysis of the shock dynamics and rear detector data. TDS performed additional analysis of the XFEL data, producing the orientation relation that was discussed and developed by TDS, APS, DD, NGJ, MGG and DR. TDS and DD drafted the manuscript. All the authors reviewed drafts and contributed towards the final manuscript.

VIII. ACKNOWLEDGEMENTS

Funding from EPSRC (EP/K0343332/1, EP/H004882/1), Rolls-Royce plc and the US De-

partment of Energy, Office of Basic Energy Sciences is acknowledged.

* tds110@ic.ac.uk; tiny.cc/tds110; Present Address: CCFE, Culham Science Centre, OX14 3DB, UK

[1] W. Kanitpanyacharoen, S. Merkel, L. Miyagi, P. Kaercher, C. Tom, Y. Wang, and H.-R. Wenk, Acta Materialia **60**, 430 (2012).

[2] D. R. Trinkle, R. G. Hennig, S. G. Srinivasan, D. M. Hatch, M. D. Jones, H. T. Stokes, R. C. Albers, and J. W. Wilkins, Physical review letters **91**, 025701 (2003).

[3] L. Young, E. Kanter, B. Krässig, Y. Li, A. March, S. Pratt, R. Santra, S. Southworth, N. Rohringer, L. DiMauro, *et al.*, Nature **466**, 56 (2010).

[4] J. Kern, R. Alonso-Mori, R. Tran, J. Hattne, R. J. Gildea, N. Echols, C. Glöckner, J. Hellmich, H. Laksmono, R. G. Sierra, *et al.*, Science **340**, 491 (2013).

[5] D. Milathianaki, S. Boutet, G. Williams, A. Higginbotham, D. Ratner, A. Gleason, M. Messerschmidt, M. M. Seibert, D. Swift, P. Hering, *et al.*, Science **342**, 220 (2013).

[6] M. Harmand, R. Coffee, M. Bionta, M. Chollet, D. French, D. Zhu, D. Fritz, H. Lemke, N. Medvedev, B. Ziaja, *et al.*, Nature Photonics **7**, 215 (2013).

[7] J. M. Silcock, Acta Metallurgica **6**, 481 (1958).

[8] S. Song and G. Gray III, Philosophical Magazine A **71**, 275 (1995).

[9] C. Greeff, D. Trinkle, and R. Albers, Journal of Applied Physics **90**, 2221 (2001).

[10] R. G. Hennig, D. R. Trinkle, J. Bouchet, S. G. Srinivasan, R. C. Albers, and J. W. Wilkins, Nature materials **4**, 129 (2005).

[11] H. R. Wenk, P. Kaercher, W. Kanitpanyacharoen, E. Zepeda-Alarcon, and Y. Wang, Physical review letters **111**, 195701 (2013).

[12] H. Zong, T. Lookman, X. Ding, C. Nisoli, D. Brown, S. R. Niezgoda, and S. Jun, Acta Materialia **77**, 191 (2014).

[13] U. F. Kocks, C. N. Tomé, and H.-R. Wenk, *Texture and anisotropy: preferred orientations in polycrystals and their effect on materials properties* (Cambridge university press, 2000).

[14] H. Zong, X. Ding, T. Lookman, J. Li, J. Sun, E. K. Cerreta, J. P. Escobedo, F. L. Addessio, and C. A. Bronkhorst, Phys. Rev. B **89**, 220101 (2014).

[15] J. Kallend, U. Kocks, A. Rollett, and H.-R. Wenk, Materials Science and Engineering: A **132**, 1 (1991).

[16] S. Herrmann, P. Hart, A. Dragone, D. Freytag, R. Herbst, J. Pines, M. Weaver, G. Carini, J. Thayer, O. Shawn, *et al.*, in *Journal of Physics: Conference Series*, Vol. 493 (IOP Publishing, 2014) p. 012013.

[17] T. Ungár, Scripta Materialia **51**, 777 (2004).

[18] Y. Zhao, J. Zhang, C. Pantea, J. Qian, L. L. Daemen, P. A. Rigg, R. S. Hixson, G. T. Gray, Y. Yang, L. Wang, Y. Wang, and T. Uchida, Phys. Rev. B **71**, 184119 (2005).

[19] G. Kaschner, C. Tomé, I. Beyerlein, S. Vogel, D. Brown, and R. McCabe, Acta materialia **54**, 2887 (2006).

[20] P. Rigg, R. Saavedra, and R. Scharff, in *Journal of Physics: Conference Series*, Vol. 500 (IOP Publishing, 2014) p. 032014.

[21] J. T. Larsen and S. M. Lane, Journal of Quantitative Spectroscopy and Radiative Transfer **51**, 179 (1994).

[22] S. P. Lyon and J. D. Johnson, Los Alamos National Laboratory, Los Alamos, NM, LA-UR-92-3407 (1992).

[23] L. Wei, L. Baosheng, W. Liping, J. Zhang, and Z. Yusheng, Journal of Applied Physics **104** (2008).

[24] D. Kazakov, O. Kozelkov, A. Mayorova, S. Malyugina, S. Mokrushin, and A. Pavlenko, in *EPJ Web of Conferences*, Vol. 94 (EDP Sciences, 2015) p. 02021.

[25] D. R. Trinkle, *A theoretical study of the HCP to omega martensitic phase transition in titanium*, Ph.D. thesis, Ohio State University (2003).

[26] D. Asenjo, F. Paillusson, and D. Frenkel, Physical review letters **112**, 098002 (2014).